Lipid engineering combined with systematic metabolic engineering of Saccharomyces cerevisiae for high-yield production of lycopene

Metabolic Engineering 52 (2019) 134–142

Contents lists available at ScienceDirect

Metabolic Engineering

journal homepage: www.elsevier.com/locate/meteng

Lipid engineering combined with systematic metabolic engineering of *Saccharomyces cerevisiae* for high-yield production of lycopene

Tian Ma[a], Bin Shi[a], Ziling Ye[b], Xiaowei Li[a], Min Liu[a], Yun Chen[c], Jiang Xia[d], Jens Nielsen[c,e,f], Zixin Deng[a,g], Tiangang Liu[a,h,*]

[a] Key Laboratory of Combinatorial Biosynthesis and Drug Discovery, Ministry of Education and School of Pharmaceutical Sciences, Wuhan University, Wuhan 430072, China
[b] J1 Biotech Co., Ltd., Wuhan 430075, PR China
[c] Department of Biology and Biological Engineering, Chalmers University of Technology, SE412 96 Gothenburg, Sweden
[d] Department of Chemistry, The Chinese University of Hong Kong, Shatin, Hong Kong SAR, China
[e] Novo Nordisk Foundation Center for Biosustainability, Chalmers University of Technology, SE412 96 Gothenburg, Sweden
[f] Novo Nordisk Foundation Center for Biosustainability, Technical University of Denmark, DK2800 Kongens Lyngby, Denmark
[g] State Key Laboratory of Microbial Metabolism, Joint International Research Laboratory of Metabolic & Developmental Sciences, and School of Life Sciences and Biotechnology, Shanghai Jiao Tong University, Shanghai 200030, China
[h] Hubei Engineering Laboratory for Synthetic Microbiology, Wuhan Institute of Biotechnology, Wuhan 430075, China

ARTICLE INFO

Keywords:
Saccharomyces cerevisiae
Systematic metabolic engineering
Lipid engineering
Triacylglycerol
Lycopene

ABSTRACT

Saccharomyces cerevisiae is an efficient host for natural-compound production and preferentially employed in academic studies and bioindustries. However, *S. cerevisiae* exhibits limited production capacity for lipophilic natural products, especially compounds that accumulate intracellularly, such as polyketides and carotenoids, with some engineered compounds displaying cytotoxicity. In this study, we used a nature-inspired strategy to establish an effective platform to improve lipid oil–triacylglycerol (TAG) metabolism and enable increased lycopene accumulation. Through systematic traditional engineering methods, we achieved relatively high-level production at 56.2 mg lycopene/g cell dry weight (cdw). To focus on TAG metabolism in order to increase lycopene accumulation, we overexpressed key genes associated with fatty acid synthesis and TAG production, followed by modulation of TAG fatty acyl composition by overexpressing a fatty acid desaturase (*OLE1*) and deletion of *Seipin* (*FLD1*), which regulates lipid-droplet size. Results showed that the engineered strain produced 70.5 mg lycopene/g cdw, a 25% increase relative to the original high-yield strain, with lycopene production reaching 2.37 g/L and 73.3 mg/g cdw in fed-batch fermentation and representing the highest lycopene yield in *S. cerevisiae* reported to date. These findings offer an effective strategy for extended systematic metabolic engineering through lipid engineering.

1. Introduction

Saccharomyces cerevisiae is an efficient and preferential chassis due to the ease of genetic manipulation and the availability of extensive knowledge regarding its physiology and biochemistry (Nevoigt, 2008). With the development of synthetic biology, it has become an indispensable platform for the synthesis of various types of chemicals and natural products, some of which represent significant milestones (e.g., the drug precursor artemisinin and the biofuel farnesene) (Ajikumar et al., 2010; Meadows et al., 2016; Paddon et al., 2013). Lipophilic natural products comprise highly diverse classes of pharmaceuticals and nutraceuticals that include polyketides and

Abbreviations: ACC1, acetyl-CoA carboxylase; ACS, acetyl-CoA synthetase; ADH2, alcohol dehydrogenase; ALD6, acetaldehyde dehydrogenase; cdw, cell dry weight; CrtB, phytoene synthase; CrtE, GGPP synthase; CrtI, phytoene desaturase; DAG, diacylglycerol; DGAT, acyl-CoA:diacylglycerol acyltransferase; FLD1, Seipin; GGPP, geranylgeranyl diphosphate; HPLC, high-performance liquid chromatography; LD, lipid droplet; MVA, mevalonate; OD_{600}, optical density at 600 nm; OLE1, fatty acid desaturase; PA, phosphatidic acid; PAP, phosphatidate phosphatase; PDC, pyruvate decarboxylase; SD, standard deviation; SE, steryl ester; TAG, triacylglycerol; tHMG1, truncated 3-hydroxy-3-methylglutaryl-CoA reductase; UFA, unsaturated fatty acid; YPD, yeast extract–peptone–dextrose; YPDG, YPD medium with 1% galactose

* Corresponding author at: Key Laboratory of Combinatorial Biosynthesis and Drug Discovery, Ministry of Education and School of Pharmaceutical Sciences, Wuhan University, Wuhan 430072, China.
E-mail address: liutg@whu.edu.cn (T. Liu).

https://doi.org/10.1016/j.ymben.2018.11.009
Received 18 July 2018; Received in revised form 20 November 2018; Accepted 20 November 2018
Available online 22 November 2018

carotenoids (Meadows et al., 2016; Tan and Liu, 2016). However, non-oleaginous *S. cerevisiae* species generally display low-production capacity for and are highly sensitive to lipophilic natural compounds, especially those that accumulate intracellularly (Xie et al., 2015). Synthetic production of such molecules through traditional metabolic engineering and up scaling has proven difficult in these model hosts.

In nature, microbes have developed various strategies to cope with potentially toxic compounds. For example, small-molecule toxic and lipophilic products can be pumped from the cell interior to the extracellular space (Martinez et al., 2009; Nikaido and Vaara, 1985; Walsh, 2000), whereas large molecules are generally accumulated intracellularly in specialized compartments. The algae *Haematococcus pluvialis* can accumulate the antioxidative carotenoid astaxanthin in oil droplets (Wayama et al., 2013), with reported correlations between the lipid- and astaxanthin-biosynthesis pathways in *H. pluvialis* along with their dynamic 'co-evolution' during fermentation (Li et al., 2017). Similarly, stimulation of lycopene synthesis in the fungus *Blakeslea trispora* is accompanied by changes in lipid composition, with increases in both lipid content and the degree of desaturation degree of neutral-lipid fatty acids (Tereshina et al., 2010). These findings suggest that some microbes are capable of producing large amounts of oil, which can be stored in lipid droplets (LDs) in order to avoid their associated toxicity. Previous studies reported efforts to improve carotenoid synthesis in the oleaginous organism *Yarrowia lipolytica*, with Gao et al. (2017) reporting production of 4 g/L β-carotene in *Y. lipolytica* through traditional metabolic engineering. Additionally, Larroude et al. (2017) reported a positive correlation between β-carotene and lipid content following production of 6.5 g/L β-carotene in *Y. lipolytica*.

LDs have a lipophilic core of neutral lipids that stores metabolic energy, thereby making them hubs for lipid metabolism. Triacylglycerols (TAGs) are water-insoluble fatty acid triesters of glycerol and the main LD components in most living organisms. In this study, we engineered a non-oleaginous *S. cerevisiae* host in order to increase the intracellular accumulation of lipophilic compounds by modulating TAG metabolism (Fig. 1). Lycopene was chosen as the intracellular lipophilic indicator, because it is a highly polyunsaturated lipophilic hydrocarbon toxic to cells at high concentrations (Klein-Marcuschamer et al., 2007; Verwaal et al., 2010), easily detectable, and a valuable compound in the food industry (Giovannucci et al., 1995; Rissanen et al., 2002). Using systematic traditional engineering methods, we established high-yield heterologous lycopene biosynthesis in *S. cerevisiae*. Additionally, context-based TAG-specific metabolic engineering was used to improve TAG accumulation, modulate TAG composition, and regulate LD size, followed by analysis of the engineered strains to evaluate the effect of the lipid platform on lycopene accumulation. Our results confirmed the successful development of an oleaginous biorefinery platform in *S. cerevisiae* that enabled the efficient overproduction of the intracellular lipophilic natural product lycopene.

2. Material and methods

2.1. Plasmids and strains

The strains used in this study are listed in Table 1. The primers used for fragments, and the fragments used for strain construction are listed in Tables S1 and S2, respectively. All fragments obtained by polymerase chain reaction were gel purified using a kit (Axygen; Corning Life Science, Corning, NY, USA) before cloning. Yeast cells were transformed using lithium acetate and PEG4000 (Gietz and Schiestl, 2007) for assembly cloning and gene deletion. Fragment assembly was performed using the Gibson method (Gibson, 2011) or yeast assembly (Gibson et al., 2008).

2.2. Media and culture conditions

S. cerevisiae CEN.PK2-1D was used as the background strain for all constructs, and *Escherichia coli* DH10B was used to propagate the recombinant plasmids. Engineered yeast strains were selected on synthetic complete medium [0.67% yeast nitrogen base with $(NH_4)_2SO_4$, 2% glucose, and appropriate amino acids] under auxotroph-screening conditions (uracil 20 mg/L, histidine 20 mg/L, tryptophan 20 mg/L, and leucine 100 mg/L) or yeast extract–peptone–dextrose (YPD) medium (2% tryptone, 1% yeast extract, and 2% glucose) with antibiotic screening (G418 200 mg/L and hygromycin 200 mg/L). All media were autoclaved at 115 °C for 30 min before use. Lycopene standards were extracted from strain L3 and purified (Zhu et al., 2015a, 2015b) (Fig. S1).

For lycopene shake-flask fermentation, recombinant yeast colonies were inoculated into 5 mL YPD medium and cultured at 30 °C on a rotary shaker (220 rpm) overnight. The seed broth (1%) was inoculated into 50 mL YPD medium. After pre-culturing, each seed culture was inoculated into 200 mL of YPDG medium (YPD medium with 1% galactose) in a 500-mL Erlenmeyer flask at an initial optical density at 600 nm (OD_{600}) of 0.5 and grown at 30 °C. Cells were harvested after

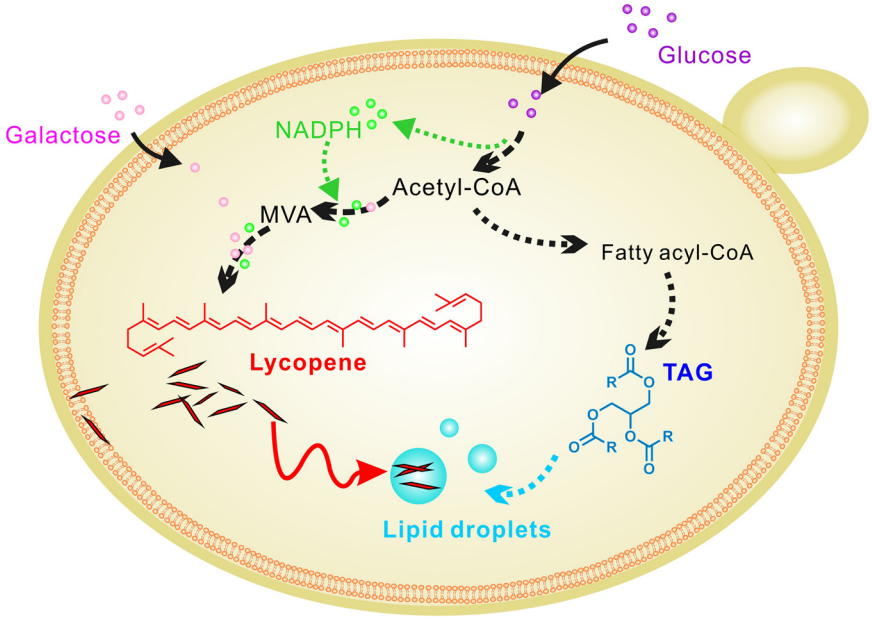

Fig. 1. Lycopene biosynthesis in *S. cerevisiae*. *S. cerevisiae* takes up glucose from the extracellular environment, and glucose metabolism results in acetyl-CoA accumulation and the release of NADPH. For lycopene production, acetyl-CoA is used in the endogenous MVA pathway and heterologous carotenoid pathway. Lycopene is distributed in lipid structures (e.g., phospholipid membranes and LDs). For TAG production, acetyl-CoA is used for endogenous fatty acid biosynthesis. TAGs are incorporated into LDs to store energy and dissolve lycopene crystals. Purple spheres represent glucose particles, pink spheres represent galactose, green spheres represent NADPH, and blue spheres represent LDs. Dotted lines represent multiple reactions.

Table 1
Strains and plasmids used in this study.

Strain	Host strain	Description	Source
S. cerevisiae CEN.PK2-1D		*MATα, ura3–52, trp1–289, leu2-3,112, his3Δ1, MAL2–8C, SUC2*	EUROSCARF
L3	*E. coli* BL21(DE3)	P_{Lac}-*AtoB-ERG13-tHMG1* P_{Lac}-*ERG12-ERG8-MVD1-Idi* P_{T7}-*CrtE-CrtB-CrtI-Idi*	(Zhu et al., 2015a)
YZL141	CEN.PK2-1D	*gal1Δ, gal7Δ, gal10Δ:: TRP1*_P_{GAL10}-*tHMG1*	This study
YZL3184	YZL141	*leu2Δ:: LEU2*_P_{GAL1}-Tm*CrtE* *ura3Δ:: HIS3*_ P_{GAL1}-Pa*CrtB*, P_{GAL10}-Bt*CrtI*	This study
YZL318496	YZL3184	*YPRCdelta15Δ:: KanMX*_P_{GAL7}-Bt*CrtI*, P_{GAL10}-Tm*CrtE*	This study
TM206	YZL3184	*XI-3Δ:: KanMX*_P_{GAL1}-*POS5*	This study
TM303	YZL3184	*X-3Δ:: HphMX*_P_{GAL1}-*ADH2*, P_{GAL10}-Se*ACS*, P_{GAL7}-*ALD6*	This study
TM115	YZL3184	*ypl062wΔ:: HphMX* *exg1Δ:: KanMX*	This study
TM606	YZL318496	*XI-3Δ::* P_{GAL1}-*POS5* *X-3Δ::* P_{GAL1}-*ADH2*, P_{GAL10}-Se*ACS*, P_{GAL7}-*ALD6* *ypl062wΔ:: HphMX* *exg1Δ:: KanMX*	This study
TM60656	TM606	*X-4Δ:: HphMX*_P_{PGK1}-*PAH1*, P_{TEF1}-*DGA1* *X-2Δ:: KanMX*_P_{TEF1}-*ACC1*$^{S659A,\ S1157A}$	This study
TM70756	TM60656	*XII-2Δ:: HphMX*_P_{PGK1}-*OLE1*	This study
TM70456	TM60656	*fld1Δ:: HphMX*_P_{PGK1}-*OLE1*	This study

72 h or 96 h of cultivation.

2.3. Lycopene extraction and titration

For lycopene extraction, cells in 0.5 mL of culture were harvested by centrifugation at 5,000 *g* for 5 min, and the supernatants were removed completely. Glass beads (0.2 g; 0.5 mm in diameter) were added, followed by dispersal of the pellets by vortexing. The pellets were then extracted with acetone (using 1% butylated hydroxytoluene) by vortexing until residues were colorless, followed by centrifugation of solution at 13,000 *g* for 10 min. The supernatant was transferred to sample vials for high-performance liquid chromatography (HPLC) measurements, where the lycopene titer was calculated using a standard curve with an appropriate dilution factor and averaged over three replicates.

An HPLC system (Dionex UltiMate 3000; Thermo Fisher Scientific, Waltham, MA, USA) equipped with a C18 column (4.6 × 150 mm; 5 μm; Agilent Technologies, Santa Clara, CA, USA) was used to detect the 474-nm signal at 30 °C. Samples were eluted with solvent A [90% aqueous acetonitrile (HPLC grade)] and solvent B [methyl alcohol-isopropyl alcohol (3:2, v/v; HPLC grade)] using the following gradient program at a flow rate of 1.0 mL/min: 0–15 min, 100–10% solvent A and 0–90% solvent B; 15–30 min, 10% solvent A and 90% solvent B; and 30–35 min, 10–100% solvent A and 90–0% solvent B (Zhou et al., 2015). Data represent the means ± standard deviation (SD) of two or three biological replicates.

2.4. TAG quantification and determination of TAG composition

Cultured cells (0.5-mL culture) were harvested by centrifugation at 5,000 *g* for 5 min, and the supernatants were removed completely. Glass beads (0.2 g; 0.5 mm in diameter) were added, and the pellets were dispersed by vortexing. The pellets were then extracted with 1 mL of 1:1 (v/v) methanol and chloroform [with an internal standard of triheptadecanoylglycerol (Nu-chek-prep; Elysian, MN, USA)] by vortexing for 10 min. The mixture was then supplemented with 0.5 mL of ddH_2O, vortexed for 5 min, and centrifuged at 13,000 *g* for 5 min. The upper water–methanol layer was removed, and the lower chloroform layer containing the lipids was extracted again with 0.5 mL of methanol: chloroform (1:1, v/v) by vortexing for 10 min, adding 0.25 mL of ddH_2O, vortexing for 5 min, and centrifugation at 13,000 *g* for 5 min. Fifty microliters of the lower red-chloroform extract was applied to preparative thin-layer chromatography, where the components were separated by hexane/diethyl ether/acetic acid (70:30:1, v/v/v) and detected using iodine. The target TAG was collected from the silica-gel plate and washed with chloroform, followed by centrifugation of the solution at 13,000 *g* for 5 min. The supernatant was transferred into a new 2-mL Eppendorf tube, and the liquid was dried with nitrogen, after which 2 mL of methanol (containing 5% sulfuric acid) and the mixture were heated at 90 °C for 2 h in sealed test tubes. One milliliter of 0.9% NaCl was added to stop the reaction, and TAGs were extracted with 300 μL of hexane by mixing and centrifugation at 13,000 *g* for 10 min, followed by transfer of the supernatant to sample vials for gas chromatography mass spectrometry (GC-MS) measurements. The GC-MS system (TSQ Quantum XLS; Thermo Fisher Scientific) was fitted with a TR-5MS capillary column (30 m × 0.25 mm × 0.25 μm; Thermo Fisher Scientific) and used helium as the carrier gas. An initial column temperature of 100 °C was maintained for 3 min, after which it was increased at 10 °C/min to 240 °C and maintained for 8 min. The inlet temperature was set to 240 °C. Data represent the means ± SD of two or three biological replicates.

2.5. Microscopic observation of lycopene distribution in yeast cells

Strains were cultivated on YPDG agar medium at 30 °C for 3 days, after which cells were scraped and diluted with 10 mM piperazine-N,N′-bis(2-ethanesulfonic acid) buffer. Images were acquired with an Ultra VIEW VoX confocal system (Perkin Elmer, Waltham, MA, USA) mounted on an Olympus IX81 microscope (Olympus, Tokyo, Japan). Fluorescence excitation was at 488 nm.

2.6. Fed-batch fermentation of the lycopene-producing strain

To create the seed culture, several single colonies of the lycopene-producing strain were grown in 5 mL YPD medium overnight at 30 °C in a rotary shaker at 220 rpm, after which 1% of the seed culture was transferred to a 500-mL flask containing 200 mL YPD and cultured at 30 °C with shaking at 220 rpm for 16–18 h. 10% of the seed culture was then inoculated into 3 L YPD medium in a 7-L fermenter for fed-batch fermentation at 30 °C, with the pH maintained at 5.5 using 2 M NaOH. Fermentation was performed at an agitation speed of between 300 rpm and 600 rpm and an airflow rate ranging from 0.5 vvm to 2 vvm.

We employed a two-stage fed-batch strategy. In the first stage, a feeding solution containing 500 g/L glucose and 15 g/L yeast extract was used to achieve rapid cell growth. Following decreases in glucose concentration to ~1 g/L in the batch culture, feeding was started in

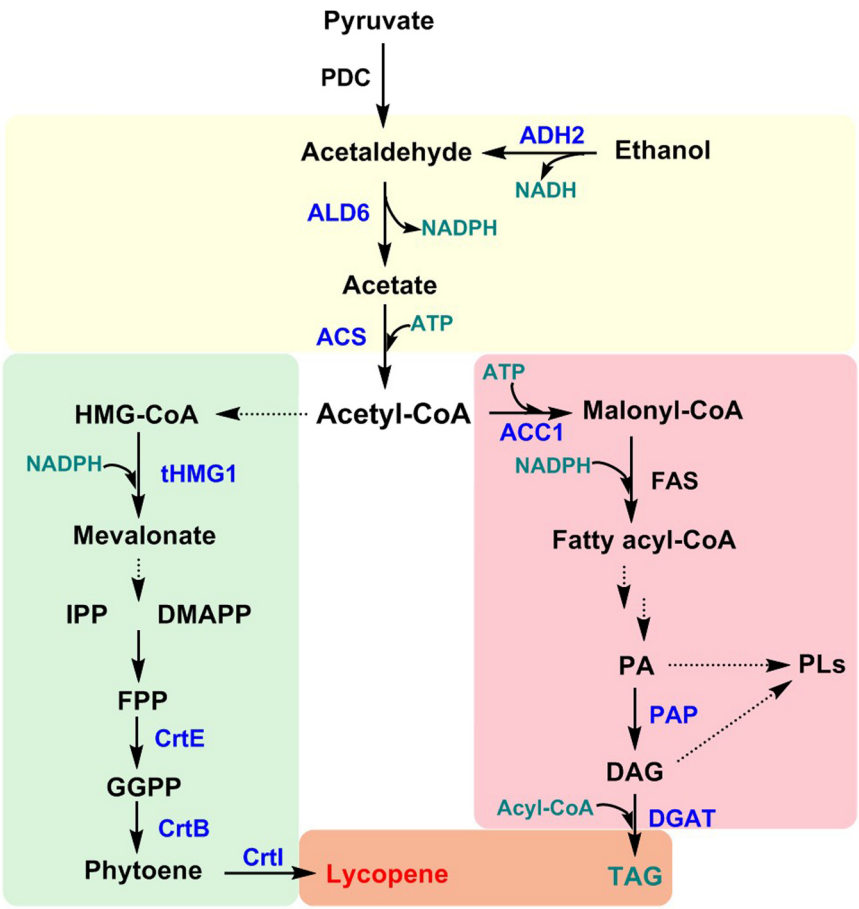

Fig. 2. Simplified schematic representation of key fluxes in lycopene biosynthesis coupled with TAG metabolism in *S. cerevisiae*. The acetyl-CoA-producing pathway is highlighted in a yellow rectangle. Reactions associated with TAG synthesis are highlighted in a red rectangle. Lycopene-biosynthetic flux is highlighted in a green rectangle. PDC, pyruvate decarboxylase; ADH2, alcohol dehydrogenase; ALD6, acetaldehyde dehydrogenase; ACS, acetyl-CoA synthetase; tHMG1, truncated 3-hydroxy-3-methylglutaryl-CoA reductase; CrtE, geranylgeranyl diphosphate synthase; CrtB, phytoene synthase; CrtI, phytoene desaturase; ACC1, acetyl-CoA carboxylase; FAS, fatty acyl-CoA synthetases; PAP, phosphatidate phosphatase; DGAT, acyl-CoA: diacylglycerol acyltransferase. HMG-CoA, 3-hydroxy-3-methyl-glutaryl-CoA; IPP, isopentenyl diphosphate; DMAPP, dimethylallyl diphosphate; FPP, farnesyl diphosphate; GGPP, geranylgeranyl diphosphate; PA, phosphatidic acid; PLs, phospholipids; DAG, diacylglycerol; TAG, triacylglycerol.

order to maintain the residual glucose concentration at between 1 g/L and 2 g/L. When the cell mass began to slowly increase (to stationary phase), the first stage was stopped, and the inducer galactose was added to a final concentration of 10 g/L. In the second stage, the feeding solution ethanol was used to produce lycopene, with the feeding rate adjusted in order to maintain the ethanol concentration at ~5 g/L. When the color of the culture changed, we detected the product in order to assess lycopene accumulation. When the lycopene concentration stopped increasing, fermentation was stopped.

3. Results

3.1. Traditional systematic metabolic engineering of lycopene biosynthesis in S. cerevisiae

To construct a strain capable of high-level lipophilic compound production and accumulation, we developed a lycopene-overproducing *S. cerevisiae* strain via six traditional metabolic engineering steps (Fig. 2): 1) enhancement of the endogenous upstream mevalonate (MVA) pathway, 2) heterologous expression of lycopene-producing enzymes, 3) enhancement of acetyl-CoA-precursor production, 4) regeneration of the redox cofactor NADPH, 5) tuning of heterologous expression of lycopene-synthesis genes, and 6) knocking out functional-bypass genes that influence carotenoid accumulation. To allow effective control of lycopene production, the genes responsible for lycopene synthesis were placed under the control of the galactose-regulated GAL promoter. Genes encoding GAL1, GAL7, and GAL10 were deleted (*gal1Δgal7Δgal10Δ*) in order to employ the GAL promoter, because *gal1Δgal7Δgal10Δ* strains do not utilize galactose.

3.1.1. Engineering of the key step in the MVA pathway

The MVA pathway provides precursors for the lycopene-synthesis pathway. Endogenous truncated 3-hydroxy-3-methylglutaryl coenzyme A reductase (tHMG1) (Donald et al., 1997), the key enzyme in the MVA pathway, was overexpressed to enhance biosynthesis of the precursor geranylgeranyl diphosphate (GGPP) for lycopene synthesis (Fig. 2). The engineered strain was called YZL141 (Table 1).

3.1.2. Construction of the heterologous lycopene pathway

S. cerevisiae does not naturally produce carotenoids. We established a heterologous lycopene pathway in strain YZL141 (Fig. 2) by genomic integration of genes encoding GGPP synthase (CrtE), phytoene synthase (CrtB), and phytoene desaturase (CrtI) from different sources. The resulting strain (YZL3184) in which *gal1*, *gal7*, and *gal10* were deleted and overexpressing *tHMG1* and *crtE* from *Taxus x media* (Ding et al., 2014), *crtB* from *Pantoea agglomerans*, and *crtI* from *B. trispora* (Chen et al., 2016) produced 4.9 mg/g cell dry weight (cdw) lycopene after 72 h of shake-flask cultivation in YPDG medium. YZL3184 was the reference strain used for subsequent engineering steps.

3.1.3. Engineering the supply of the acetyl-CoA precursor

Acetyl-CoA serves as the substrate for lycopene biosynthesis and a building block for the upstream pathway of fatty acid synthesis. In *S. cerevisiae*, activation of acetate is the only cytosolic route for producing acetyl-CoA. During growth on glucose, the high glycolytic flux is directed toward ethanol formation (Pronk et al., 1996); therefore, it is necessary to redirect the carbon flux from ethanol to acetyl-CoA in the cytosolic compartment. Overexpression of *acetaldehyde dehydrogenase ALD6* (Shiba et al., 2007) and *acetyl-CoA synthetase ACS* from *Salmonella enterica* substantially increases target downstream flux. By combining this strategy with overexpression of *alcohol dehydrogenase ADH2*, the

only step responsible for oxidizing ethanol to acetaldehyde (Chen et al., 2013) (Fig. 2), we directed ethanol toward acetyl-CoA production in strain TM303 engineered from strain YZL3184. This further improved lycopene production to 10.3 mg/g cdw.

3.1.4. Engineering of NADPH generation

Engineering metabolism by targeting redox cofactors, such as NADP (H), can be used to suppress anabolism (Matsuda et al., 2013). In *S. cerevisiae*, the NADH kinase POS5, which mediates the ATP-driven conversion of NADH to NADPH appears dominant (Outten and Culotta, 2003). In the present study, we overexpressed *POS5* in order to promote intracellular generation of the cofactors in order to optimize metabolic output. The resulting strain (TM206) yielded 11.9 mg/g cdw lycopene, a two-fold increase relative to that of the reference strain YZL3184.

3.1.5. Tuning of heterologous crt expression in the downstream pathway

To balance and optimize lycopene-biosynthetic flux, expression of the *crt* genes was tuned by adjusting the integrated copy numbers. When one additional copy of *crtE* and *crtI* were integrated, lycopene production in the resulting strain (YZL318496) increased to 26.5 mg/g cdw, a four-fold increase relative to that of the reference strain YZL3184 (more information in Supplementary materials Fig. S2).

3.1.6. Knockout of bypass-pathway genes to increase lycopene accumulation

Previous studies suggest that deletion of certain genes in the bypass pathway can improve carotenoid overproduction. For example, knockout of *ypl062w* reportedly enhances carotenoid production by increasing intracellular acetyl-CoA, which enhances MVA-pathway flux and, consequently, lycopene production (Chen et al., 2016). Moreover, knockout of *exg1* promotes carotenoid production in yeast BY4741 (Trikka et al., 2015). In the present study, we knocked out both *ypl062w* and *exg1* in YZL3184 to construct strain TM115, which produced lycopene at 34.4 mg/g cdw.

Combining all of the strategies described resulted in generation of the lycopene-overproducing strain TM606, which produced 43.7 mg lycopene/g cdw, an 8.9-fold increase relative to that of YZL3184. When the cultivation time was prolonged to 96 h, the yield reached 56.2 mg/g cdw (Fig. 3B), which exceeded that of previously reported yields in *S. cerevisiae* (Chen et al., 2016; Xie et al., 2014).

To investigate lycopene accumulation in yeast cells, each strain was observed by confocal microscopy. In the cells of strain YZL3184, we found that most of the lycopene accumulated in LDs (Fig. S3). Additionally, we observed that lycopene distribution differentiated between the various engineered strains, and that in TM606 cells, lycopene was dispersed throughout the cytoplasm (Fig. 3C).

3.2. Engineering of TAG biosynthesis to increase TAG content and lycopene accumulation

As a lipophilic carotenoid, β-carotene accumulates in lipid bodies in *Dunaliella* algae (Katz et al., 1995). Additionally, the oleaginous yeast *Y. lipolytica* can accumulate up to 90 mg β-carotene/g cdw in dark-colored drops (Larroude et al., 2017). Similarly, in the present study, we observed that lycopene produced in *S. cerevisiae* accumulated in LDs (Fig. S3), and that increasing production resulted in lycopene dispersal throughout the cytoplasm. Because lipid production in *S. cerevisiae* is lower than that in oleaginous hosts, we hypothesized that lipid production aids in the accumulation of intracellular lipophilic products, such as lycopene, in microorganisms. To investigate the correlation between lipid and lycopene syntheses, we engineered the metabolism of TAG, the predominant neutral lipid of LD cores.

In *S. cerevisiae*, TAGs are synthesized from phosphatidic acid (PA) and diacylglycerol (DAG) by two key enzymes, phosphatidate phosphatase (PAP) and acyl-CoA:diacylglycerol acyltransferase (DGAT). PAP, encoded by *PAH1*, catalyzes the conversion of PA into DAG, which is the crucial step in TAG synthesis (Oludotun et al., 2011). DGAT, encoded by *DGA1*, catalyzes DAG acylation, the final and only committed step in TAG biosynthesis (Sorger and Daum, 2003) (Fig. 2). The starting molecule of TAG biosynthesis, acetyl-CoA, is the central metabolite in fatty acid biosynthesis. Acetyl-CoA carboxylase (ACC1) is responsible for the carboxylation of acetyl-CoA to form malonyl-CoA, the first committed and critical step in fatty acid metabolism. The introduction of two point mutations in ACC1 at Ser659 and Ser1157 results in a three-fold enhancement of ACC1 activity and increased total fatty acid content (Shi et al., 2014). Therefore, we engineered the high-

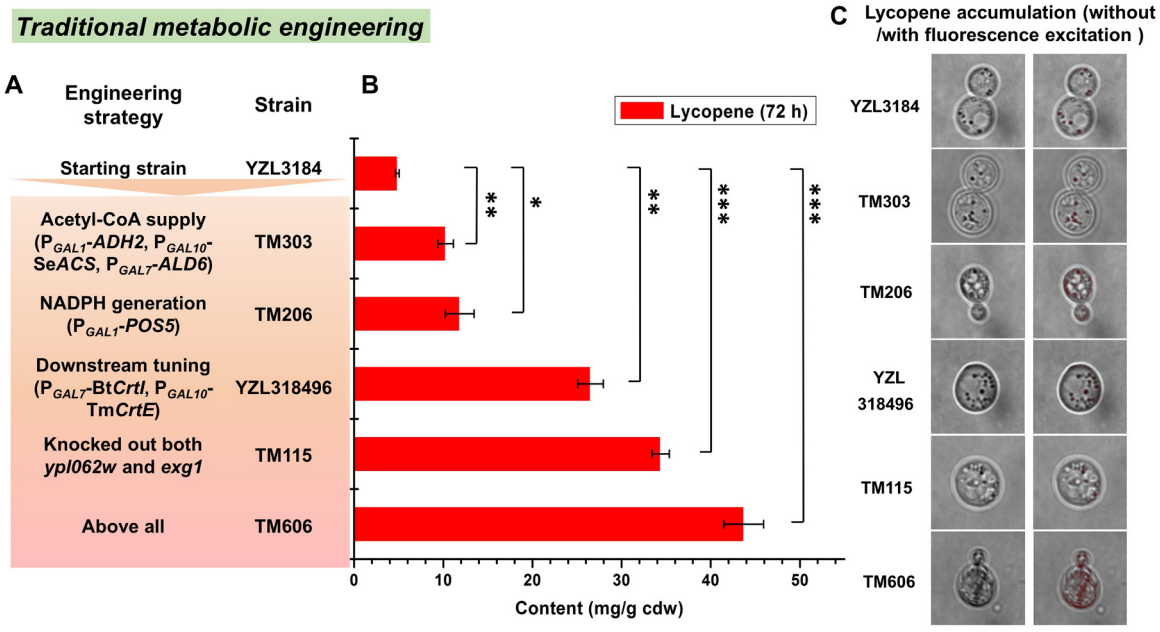

Fig. 3. Steps of traditional systematic metabolic engineering of lycopene synthesis. (*A*) Traditional metabolic engineering strategies. (*B*) Accumulation of lycopene in different strains. $^{*}P < 0.05$; $^{**}P < 0.01$; $^{***}P < 0.001$ (Student's *t*-test: two-tailed, two-sample equal variance). (*C*) Lycopene distribution in strains exhibiting different levels of accumulation. Results in the presence (right) and absence (left) of fluorescence excitation at 488 nm.

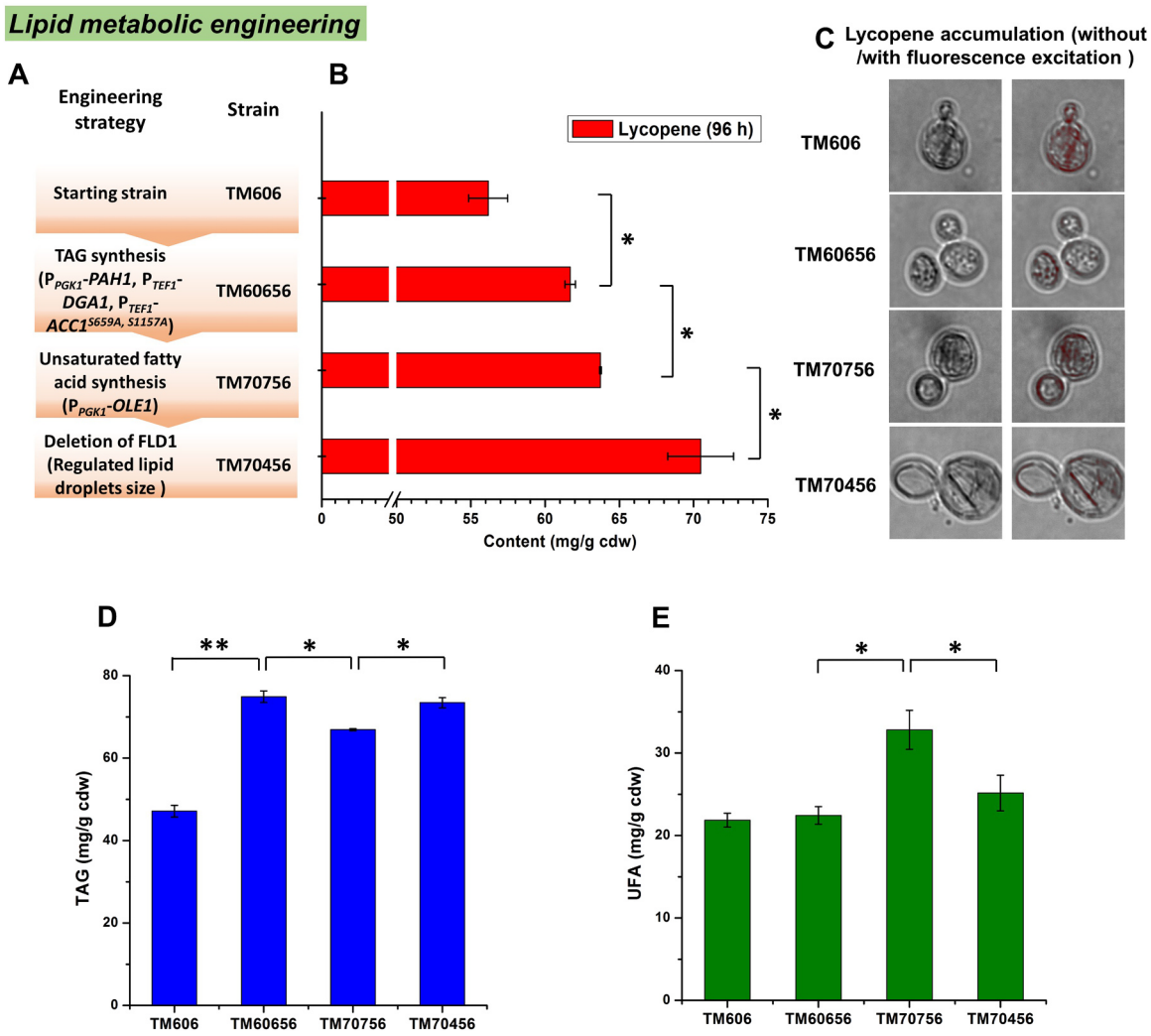

Fig. 4. Metabolic engineering of lipid synthesis in the lycopene-producing strain TM606. (*A*) Lipid metabolic engineering strategies. (*B*) Lycopene accumulation. (*C*) Lycopene distribution in strains exhibiting different levels of accumulation. Results in the presence (right) and absence (left) of fluorescence excitation at 488 nm. (*D*) TAG accumulation. (*E*) UFA composition in TAGs. $^{*}P < 0.05$; $^{**}P < 0.01$. (Student's *t*-test: two-tailed, two-sample equal variance).

yield lycopene-producing strain TM606 to overproduce TAGs by overexpressing the three key enzymes, endogenous *PAH1*, *DGA1*, and a mutated *ACC1* variant encoding $ACC1^{S659AS1157A}$, under the control of the strong constitutive promoters P_{PGK1} and P_{TEF1}. The resulting strain (TM60656) displayed increased TAG production of 74.9 mg/g cdw (Fig. 4D) and increased lycopene production of 61.7 mg/g cdw (Fig. 4B), with the lycopene in most of the TM60656 cells observed in droplets rather than dispersed throughout the cytoplasm (Fig. 4C). These results indicated that increasing TAG production significantly promoted increased lycopene accumulation.

3.3. Engineering the production of unsaturated TAGs to increase lycopene accumulation

The fatty acyl chains utilized in TAG biosynthesis are mainly derived from fatty acid biosynthesis in lipid biosynthesis, with incorporation of different types of fatty acid chains ultimately determining TAG composition. A previous study reported that increasing the exogenous supply of unsaturated fatty acids (UFAs), such as oleic acid (C18:1) and palmitoleic acid (C16:1), can efficiently increase β-carotene accumulation (Sun et al., 2016). In the present study, we hypothesized that the types of fatty acid chains present in TAGs might affect lycopene solubility.

The *OLE1* gene encodes the Δ9 fatty acid desaturase, which is involved in UFA production in *S. cerevisiae* by catalyzing the insertion of a double bond between carbons nine and ten of the saturated fatty acyl substrates palmitoyl (C16:0)- and stearoyl (C18:0)-CoA to yield the monoenoic products palmitoleic (C16: l) and oleic (C18: l) acid (Stukeys et al., 1990). In the present study, we overexpressed endogenous *OLE1* in strain TM60656 to produce TM70756, which generated 66.9 mg TAGs/g cdw. Moreover, we found that the UFA substrates of TAGs increased to 32.8 mg/g cdw, and lycopene accumulation increased to 63.7 mg/g cdw (Fig. 4B). These results indicated that enhancing UFA biosynthesis represents an efficacious strategy for improving the production of polyene-lipophilic products in recombinant *S. cerevisiae*.

3.4. Deletion of FLD1 improves lycopene accumulation

In addition to LD composition, regulating LD size represents another important strategy for enhancing lycopene accumulation in LDs. FLD1 regulates the cellular dynamics of LDs, and *FLD1* deletion in *S. cerevisiae* increases lipid levels, LD clustering, and the formation of enlarged LDs (Fei et al., 2008). Additionally, formation of "supersized" LDs up to 50-fold larger than the normal volume was observed in FLD1-depleted cells (Sorger and Daum, 2002). In the present study, *FLD1* deletion in strain TM70756 to create TM70456 resulted in increased TAG production at 73.5 mg/g cdw and increased lycopene accumulation to 70.5 mg/g cdw (Fig. 4B). And the cells harbored lycopene with a needle-like

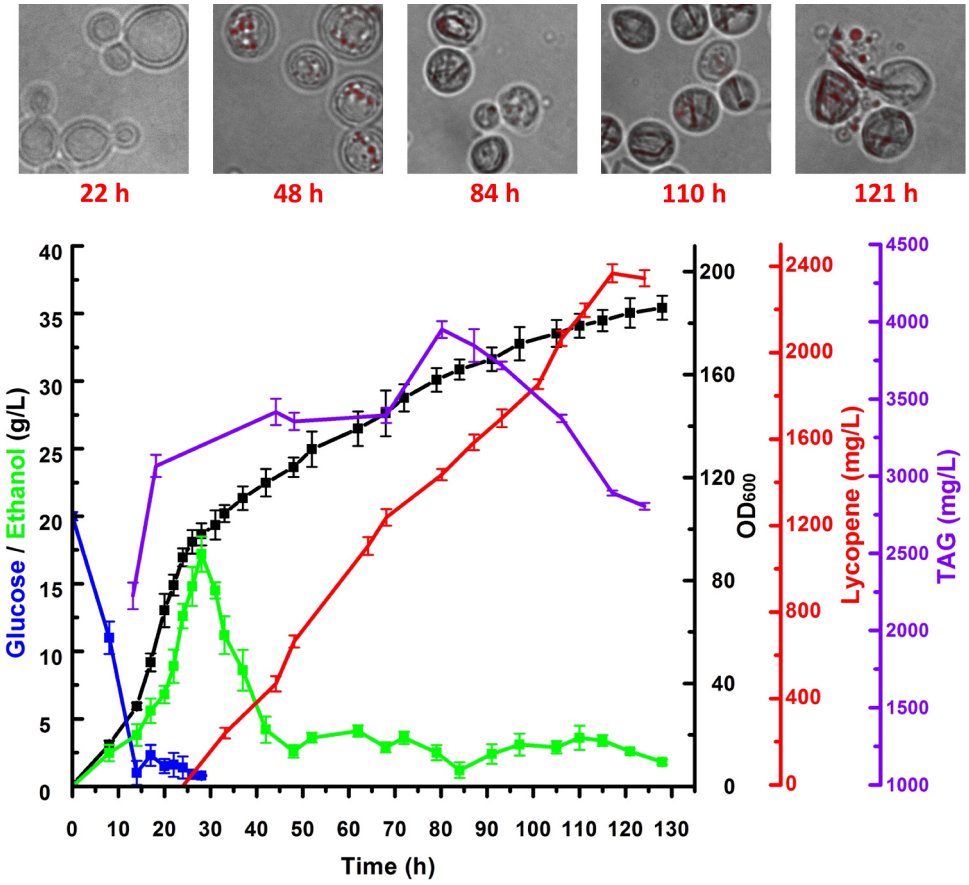

Fig. 5. High-density fermentation for lycopene production. Time courses showing changes in cell growth, lycopene and TAG production, and the micro-morphology of TM70456 cells during fed-batch fermentation.

morphology (Fig. 4C). Our results indicated that we successfully developed an efficient lipid platform through manipulating TAG content and UFA composition and regulating LD size in a high-yield lycopene-producing strain, which resulted in a 25% increase in lycopene production. To the best of our knowledge, this represents the highest yield of lycopene in *S. cerevisiae* reported to date.

3.5. High-density fermentation for lycopene production

We used two stages of cell growth and product accumulation during high-density cell fermentation, with these stages separated by employing a modified GAL-regulation system and controlling the supply of the carbon source. After first-stage feeding, the biomass reached an OD_{600} of 98 after 28 h, with no observed changes in cell color. During the second feeding stage involving ethanol, we observed TAG accumulation initially increased, and decreased in mid-to-late stage of fermentation. Lycopene accumulation dramatically increased, although the biomass increased only slightly, and the morphology of lycopene in cells changed from small droplets to needle-like structure. The results showed that lycopene accumulated continuously to 2.37 g/L and 73.3 mg/g cdw until the completion of fermentation (Fig. 5). These results demonstrated the accumulation of lycopene content much higher than those reported previously in engineered *S. cerevisiae* strains (Chen et al., 2016; Xie et al., 2015) or in natural lycopene producers, such as tomato (Agarwal et al., 2001) and *B. trispora* (Mantzouridou and Tsimidou, 2008).

4. Discussion

The overproduction of the lipophilic natural product lycopene, which accumulates intracellularly upon overproduction in microbial hosts, is limited by cell-storage capacity or cell cytotoxicity, thereby hampering the up scaling of production processes. The TAG-rich chassis constructed in this study allowed high-yield overproduction of lycopene in *S. cerevisiae*. We developed a yeast platform by manipulating three main factors determining the production of TAGs, which form the core of LDs: overexpression of key genes associated with fatty acid synthesis and TAG production, engineering TAG composition, and regulating LD size. The platform showed a 25% increase in lycopene production relative to that of the high-yield strain used as the starting host. These findings showed that improving the lipid-biosynthesis network promoted increased production of intracellular lycopene in *S. cerevisiae*.

Interestingly, we observed that the three steps in TAG engineering cooperated to determine TAG composition and content. Strain TM606, generated to study the relationship between TAG metabolism and lycopene production, produced 47.1 mg TAGs/g cdw, with UFAs accounting for 21.9 mg/g cdw. In the first step of TAG engineering (TM60656), TAG content increased to 59%, whereas UFA composition comprised only 30% of the TAG profile, which was similar to that observed in the starting strain and implied that TAG production increased in this step primarily through enhanced synthesis of saturated fatty acids. Additionally, lycopene accumulation increased 10% ($P < 0.05$) during this step. Moreover, our use of a strategy involving overexpression of *PAH1*, *DGA1*, and the mutant form of *ACC1* was based on a method described previously (Ferreira et al., 2018) and resulted in production of 129 mg TAG/g cdw. We speculated that the lycopene-biosynthesis pathway shared the same TAG precursor (acetyl-CoA), which resulted in lower TAG accumulation. In the second engineering step, UFA comprised 49% of the TAG profile (a 46% increase), whereas total TAG content decreased by 11% ($P < 0.05$), suggesting that

overexpressing *OLE1* in order to increase UFA content not only influenced TAG composition but also slightly decreased TAG accumulation; however, lycopene accumulation during this step also increased. This result suggested that the double-bond structure between UFAs and lycopene promoted lycopene accumulation in TAGs. Recently, it was also found that greater lipid unsaturation led to increased cellular respiratory activity (Budin et al., 2018). In the third engineering step, *FLD1* deletion increased TAG accumulation by 10% increase ($P < 0.05$), resulting in an 11% ($P < 0.05$) increase in lycopene accumulation. Together, these findings suggested that lycopene accumulation correlated with TAG production.

Observation of lycopene microstructure in cells enables a deeper understanding of correlations between lipid-metabolism engineering and lycopene accumulation. In the traditional engineering steps, we were able to easily identify increases in lycopene-containing droplets following increased lycopene production, until the lycopene was ultimately dispersed throughout the cells. In the engineering steps focused on lipid metabolism in TM60656, we similarly observed the storage of lycopene in droplets accompanied by increased lycopene production. Moreover, in most of the cells of the highest yielding strain (TM70456), we observed intracellular needle-like structures similar to lycopene crystal structures (Fig. S4). For the TAG-biosynthesis network, we engineered only a few key steps in order to provide proof-of-concept results. Previous studies showed that engineering fatty acid synthesis and TAG metabolism in *S. cerevisiae* could result in a more efficient cell factory for oil production (Ferreira et al., 2018; Zhou et al., 2016). Notably, our results confirmed that lipophilic products that share the same precursors (such as acetyl-CoA) with TAG biosynthesis should be considered in order to balance the flux to both pathways.

LDs in *S. cerevisiae* and other eukaryotes are considered reservoirs of energy and building blocks for lipid synthesis. The two most prominent neutral lipids, TAG and steryl esters (SEs), both contribute to the formation of LDs. A biophysical investigation revealed that individual neutral lipids strongly affect the internal structure of LDs, and that SEs form several ordered shells below the surface of the phospholipid monolayer of LDs, whereas TAGs are more or less randomly packed in the center of LDs (Czabany et al., 2008). Although *S. cerevisiae* contains both TAG and SEs, we preliminarily explored the effects of TAGs on intracellular lycopene accumulation. Future studies should investigate whether SE content can be appropriately tuned in order to optimize LD formation, similar to that reported previously (Ferreira et al., 2018).

FLD1 deletion can result in the accumulation of supersized LDs accompanied by increased TAG content defective lipolysis (Fei et al., 2008; Wolinski et al., 2011). In the present study, this strategy resulted in increased lycopene accumulation, as well as more cells harboring lycopene with a needle-like morphology similar to that of lycopene crystal structures. This suggested that supersized LDs provided an environment conducive to the formation of these structures, which also enhanced lycopene purification. A previous report noted that the *FLD1*-knockout phenotype decreases the life span of yeast (Fabrizio et al., 2010), which was confirmed in our results showing decreases in the OD_{600} values of the *FLD1*-knockout strain (TM70456) (Fig. S5). Future efforts at metabolic engineering might attempt other gene modification to increase LD size, such as overexpression of LDP1 (lipid droplet protein) (Zhu et al., 2015b) in order to avoid the attenuated cell growth associated with *FLD1* deletion.

This study focused on TAGs as the primary LD component and correlations between TAG content, composition, and the regulation of LDs with improved lycopene accumulation. Compared with prior attempts targeting this pathway, our findings were the first describing lipid-metabolic engineer to promote lycopene overproduction in a non-oleaginous organism. The industrialization of any product in the field of metabolic engineering is determined by titer, yield, productivity, content, purification ability, biosafety, and market acceptance. Oleaginous organism, such as *Y. lipolytica,* can produce excessive lipids for high production of β-carotene (Larroude et al., 2017) while avoiding toxicity from carotenoid accumulation. The present study optimized lipid production in order to improve lycopene accumulation, resulting in 73.3 mg/g cdw and 2.37 g/L lycopene, which represents the highest yield reported to date in oleaginous organisms or in *S. cerevisiae*, despite lycopene exhibiting higher toxicity than β-carotene. Oleaginous organisms use large quantities of glucose during lipid production, therefore, we implemented lipid production in *S. cerevisiae* by managing the efficient transfer of glucose toward pathways associated with lipid and lycopene production, thereby avoiding excessive lipid production due higher consumption of glucose and promoting a more energy efficient process. The optimal strain (TM70456) producing lycopene in needle-like structures enabled easier purification following the fermentation stage, thereby potentially decreasing the cost of separation of lycopene from large amounts of lipids in oleaginous organisms during industrial production. We believe that our strategy supports the use of non-oleaginous organisms for industrial production of such products.

Acknowledgments

This work was supported by funding from J1 Biotech Co. Ltd., Hubei Natural Science Fund Project 2017CFA054, Hubei Provincial Technical Commonweal Project 2013BKB019, and Hubei Provincial Technical Innovation Project 2017AHB068.

Conflicts of interest

T. M., B.S., Z.Y., Z.D., and T.L. have applied for a series of patents based on this work, and remaining authors declare no conflict of interest.

Appendix A. Supplementary material

Supplementary data associated with this article can be found in the online version at doi:10.1016/j.ymben.2018.11.009

References

Agarwal, A., Shen, H., Agarwal, S., Rao, A.V., 2001. Lycopene content of tomato products: its stability, bioavailability and in vivo antioxidant properties. J. Med. Food 4 (1), 9–15.

Ajikumar, P., Xiao, W., Tyo, K., Wang, Y., Simeon, F., Leonard, E., Mucha, O., Too, H., Pfeifer, B., Stephanopoulos, G., 2010. Isoprenoid pathway optimization for taxol precursor overproduction in *Escherichia coli*. Science 330, 70–74.

Budin, I., de Rond, T., Chen, Y., Chan, L.J.G., Petzold, C.J., Keasling, J.D., 2018. Viscous control of cellular respiration by membrane lipid composition. Science. https://doi.org/10.1126/science.aat7925.

Chen, Y., Daviet, L., Schalk, M., Siewers, V., Nielsen, J., 2013. Establishing a platform cell factory through engineering of yeast acetyl-CoA metabolism. Metab. Eng. 15 (1), 48–54.

Chen, Y., Xiao, W., Wang, Y., Liu, H., Li, X., Yuan, Y., 2016. Lycopene overproduction in *Saccharomyces cerevisiae* through combining pathway engineering with host engineering. Microb. Cell Fact. 15, 113.

Czabany, T., Wagner, A., Zweytick, D., Lohner, K., Leitner, E., Ingolic, E., Daum, G., 2008. Structural and biochemical properties of lipid particles from the yeast *Saccharomyces cerevisiae*. J. Biol. Chem. 283 (25), 17065.

Ding, M., Yan, H., Li, L., Zhai, F., Shang, L., Yin, Z., Yuan, Y., 2014. Biosynthesis of taxadiene in *Saccharomyces cerevisiae*: selection of geranylgeranyl diphosphate synthase directed by a computer-aided docking strategy. PLoS One 9 (10), e109348.

Donald, K., Hampton, R., Fritz, I., 1997. Effects of overproduction of the catalytic domain of 3-hydroxy-3-methylglutaryl coenzyme A reductase on squalene synthesis in *Saccharomyces cerevisiae*. Appl. Environ. Microbiol. 63 (9), 3341–3344.

Fabrizio, P., Hoon, S., Shamalnasab, M., Galbani, A., Wei, M., Giaever, G., Nislow, C., Longo, V., 2010. Genome-wide screen in *Saccharomyces cerevisiae* identifies vacuolar protein sorting, autophagy, biosynthetic, and tRNA methylation genes involved in life span regulation. PLoS Genet. 6 (7), 60–67.

Fei, W., Shui, G., Gaeta, B., Du, X., Kuerschner, L., Li, P., Yang, H., 2008. Fld1p, a functional homologue of human seipin, regulates the size of lipid droplets in yeast. J. Cell Biol. 180 (3), 473–482.

Ferreira, R., Teixeira, P.G., Gossing, M., David, F., Siewers, V., Nielsen, J., 2018. Metabolic engineering of *Saccharomyces cerevisiae* for overproduction of triacylglycerols. Metab. Eng. Commun. 6, 22–27.

Gao, S., Tong, Y., Zhu, L., Ge, M., Zhang, Y., Chen, D., Jiang, Y., Yang, S., 2017. Iterative integration of multiple-copy pathway genes in *Yarrowia lipolytica* for heterologous β-carotene production. Metab. Eng. 41, 192–201.

Gibson, D., 2011. Enzymatic assembly of overlapping DNA fragments. Methods Enzymol. 498, 349.
Gibson, D., Benders, G., Axelrod, K., Zaveri, J., Algire, M., Moodie, M., Montague, M., Venter, C., Smith, H., Hutchison, C., 2008. One-step assembly in yeast of 25 overlapping DNA fragments to form a complete synthetic *Mycoplasma genitalium* genome. Proc. Natl. Acad. Sci. USA 105 (51), 20404–20409.
Gietz, R., Schiestl, R., 2007. Large-scale high-efficiency yeast transformation using the LiAc/SS carrier DNA/PEG method. Nat. Protoc. 2 (1), 38–41.
Giovannucci, E., Ascherio, A., Rimm, E., Stampfer, M., Colditz, G., Willett, W., 1995. Intake of carotenoids and retinol in relation to risk of prostate cancer. J. Natl. Cancer Inst. 87 (23), 1767–1776.
Katz, A., Jimenez, C., Pick, U., 1995. Isolation and characterization of a protein associated with carotene globules in the alga *Dunaliella bardawil*. Plant Physiol. 108 (4), 1657–1664.
Klein-Marcuschamer, D., Ajikumar, P., Stephanopoulos, G., 2007. Engineering microbial cell factories for biosynthesis of isoprenoid molecules: beyond lycopene. Trends Biotechnol. 25 (9), 417–424.
Larroude, M., Celinska, E., Back, A., Thomas, S., Nicaud, J.M., Ledesma-Amaro, R., 2017. A synthetic biology approach to transform *Yarrowia lipolytica* into a competitive biotechnological producer of β-carotene. Biotechnol. Bioeng. 115 (2), 464–472.
Li, K., Cheng, J., Ye, Q., He, Y., Zhou, J., Cen, K., 2017. In vivo kinetics of lipids and astaxanthin evolution in *Haematococcus pluvialis* mutant under 15% CO_2 using Raman microspectroscopy. Bioresour. Technol. 244, 1439–1444.
Mantzouridou, F., Tsimidou, M., 2008. Lycopene formation in *Blakeslea trispora*. Chemical aspects of a bioprocess. Trends Food Sci. Technol. 19 (7), 363–371.
Martinez, J., Sánchez, M., Martínezsolano, L., Hernandez, A., Garmendia, L., Fajardo, A., Alvarezortega, C., 2009. Functional role of bacterial multidrug efflux pumps in microbial natural ecosystems. FEMS Microbiol. Rev. 33 (2), 430–449.
Matsuda, F., Ishii, J., Kondo, T., Ida, K., Tezuka, H., Kondo, A., 2013. Increased isobutanol production in *Saccharomyces cerevisiae* by eliminating competing pathways and resolving cofactor imbalance. Microb. Cell Fact. 12 (1), 1–11.
Meadows, A., Hawkins, K., Tsegaye, Y., Antipov, E., Kim, Y., Raetz, L., Xu, L., 2016. Rewriting yeast central carbon metabolism for industrial isoprenoid production. Nature 537 (7622), 694–697.
Nevoigt, E., 2008. Progress in metabolic engineering of *Saccharomyces cerevisiae*. Microbiol. Mol. Biol. Rev. 72 (3), 379–412.
Nikaido, H., Vaara, M., 1985. Molecular basis of bacterial outer membrane permeability. Microbiol. Rev. 49 (1), 1–32.
Oludotun, A., Horn, P., Sungkyung, L., Binns, D., Anita, C., Chapman, K., Goodman, J., 2011. The yeast lipin orthologue Pah1p is important for biogenesis of lipid droplets. J. Cell Biol. 192 (6), 1043–1055.
Outten, C., Culotta, V., 2003. A novel NADH kinase is the mitochondrial source of NADPH in *Saccharomyces cerevisiae*. EMBO J. 22 (9), 2015–2024.
Paddon, C., Westfall, P., Pitera, D., Benjamin, K., Fisher, K., Mcphee, D., Leavell, M., Tai, A., Main, A., Eng, D., 2013. High-level semi-synthetic production of the potent antimalarial artemisinin. Nature 496 (7446), 528–532.
Pronk, J., Yde, S., Van Dijken, J., 1996. Pyruvate metabolism in *Saccharomyces cerevisiae*. Yeast 12 (16), 1607–1633.
Rissanen, T., Voutilainen, S., Nyyssönen, K., Salonen, J., 2002. Lycopene, atherosclerosis, and coronary heart disease. Exp. Biol. Med. 227 (10), 900–907.
Shi, S., Chen, Y., Siewers, V., Nielsen, J., 2014. Improving production of malonyl coenzyme A-derived metabolites by abolishing Snf1-dependent regulation of *acc1*. mBio 5 (3) (01130-01114).
Shiba, Y., Paradise, E., Kirby, J., Ro, D., Keasling, J., 2007. Engineering of the pyruvate dehydrogenase bypass in *Saccharomyces cerevisiae* for high-level production of isoprenoids. Metab. Eng. 9 (2), 160–168.
Sorger, D., Daum, G., 2002. Synthesis of triacylglycerols by the acyl-coenzyme A: diacylglycerol acyltransferase Dga1p in lipid particles of the yeast *Saccharomyces cerevisiae*. J. Bacteriol. 184 (2), 519–524.
Sorger, D., Daum, G., 2003. Triacylglycerol biosynthesis in yeast. Appl. Microbiol. Biot. 61 (4), 289–299.
Stukeys, J., McDonough, V., Martin, C., 1990. The *OLE1* gene of *Saccharomyces cerevisiae* encodes the Δ9 fatty acid desaturase and can be functionally replaced by the rat stearoyl-CoA desaturase gene. J. Biol. Chem. 265 (25), 20144–20149.
Sun, Y., Sun, L., Shang, F., Yan, G., 2016. Enhanced production of β-carotene in recombinant *Saccharomyces cerevisiae* by inverse metabolic engineering with supplementation of unsaturated fatty acids. Process Biochem. 51 (5), 568–577.
Tan, G., Liu, T., 2016. Rational synthetic pathway refactoring of natural products biosynthesis in actinobacteria. Metab. Eng. 39, 228–236.
Tereshina, V., Memorskaya, A., Feofilova, E., 2010. Lipid composition of the mucoraceous fungus *Blakeslea trispora* under lycopene formation-stimulating conditions. Microbiology 79 (1), 34–39.
Trikka, F., Nikolaidis, A., Athanasakoglou, A., Andreadelli, A., Ignea, C., Kotta, K., Argiriou, A., Kampranis, S., Makris, A., 2015. Iterative carotenogenic screens identify combinations of yeast gene deletions that enhance sclareol production. Microb. Cell Fact. 14, 60.
Verwaal, R., Jiang, Y., Wang, J., Daran, J., Sandmann, G., Ja, V., Van Ooyen, A., 2010. Heterologous carotenoid production in *Saccharomyces cerevisiae* induces the pleiotropic drug resistance stress response. Yeast 27 (12), 983–998.
Walsh, C., 2000. Molecular mechanisms that confer antibacterial drug resistance. Nature 406 (6797), 775–781.
Wayama, M., Ota, S., Matsuura, H., Nango, N., Hirata, A., Kawano, S., 2013. Three-dimensional ultrastructural study of oil and astaxanthin accumulation during encystment in the green alga *Haematococcus pluvialis*. PLoS One 8 (1), e53618.
Wolinski, H., Kolb, D., Hermann, S., Koning, R., Kohlwein, S., 2011. A role for seipin in lipid droplet dynamics and inheritance in yeast. J. Cell Sci. 124 (22), 3894–3904.
Xie, W., Liu, M., Lv, X., Lu, W., Gu, J., Yu, H., 2014. Construction of a controllable β-carotene biosynthetic pathway by decentralized assembly strategy in *Saccharomyces cerevisiae*. Biotechnol. Bioeng. 111 (1), 125–133.
Xie, W., Ye, L., Lv, X., Xu, H., Yu, H., 2015. Sequential control of biosynthetic pathways for balanced utilization of metabolic intermediates in *Saccharomyces cerevisiae*. Metab. Eng. 28, 8–18.
Zhou, P., Ye, L., Xie, W., Lv, X., Yu, H., 2015. Highly efficient biosynthesis of astaxanthin in *Saccharomyces cerevisiae* by integration and tuning of algal crtZ and bkt. Appl. Microbiol. Biot. 99 (20), 8419–8428.
Zhou, Y., Buijs, N., Zhu, Z., Qin, J., Siewers, V., Nielsen, J., 2016. Production of fatty acid-derived oleochemicals and biofuels by synthetic yeast cell factories. Nat. Commun. 7, 11709.
Zhu, F., Lu, L., Fu, S., Zhong, X., Hu, M., Deng, Z., Liu, T., 2015a. Targeted engineering and scale up of lycopene overproduction in *Escherichia coli*. Process Biochem. 50, 341–346.
Zhu, Z., Ding, Y., Gong, Z., Yang, L., Zhang, S., Zhang, C., Lin, X., Shen, H., Zou, H., Xie, Z., 2015b. Dynamics of the lipid droplet proteome of the oleaginous yeast *Rhodosporidium toruloides*. Eukaryot. Cell 14 (3), 252–264.